OKU Fen Bilimleri Enstitüsü Dergisi
6(Ek Sayı): 555-566, 2023

OKU Journal of The Institute of Science and Technology,
6(Special Issue): 555-566, 2023

Osmaniye Korkut Ata Üniversitesi Fen Bilimleri Enstitüsü Dergisi

Osmaniye Korkut Ata University Journal of The Institute of Science and Technology

Yarı Küresel Burunlu Torpido Benzeri Geometri Etrafındaki Akışın POD Analizi

Ömer KENAN[1], Bülent YANIKTEPE[2]*, Ertugrul SEKEROGLU[3], Muammer OZGOREN[4], Ezgi AKBUDAK[5], Tahir DURHASAN[6], Alpaslan KILAVUZ[7], Besir SAHIN[8], Huseyin AKILLI[9], Levent Ali KAVURMACIOGLU[10]

[1,2,3,5]Osmaniye Korkut Ata Üniversitesi, Mühendislik Fakültesi, Enerji Sistemleri Mühendisliği Bölümü, 80000, Osmaniye
[4]Necmettin Erbakan Üniversitesi, Havacılık ve Uzay Bilimleri Fakültesi, Uçak Mühendisliği Bölümü, 42000, Konya
[6]Adana Alparslan Türkeş Bilim ve Teknoloji Üniversitesi, Havacılık ve Uzay Bilimleri Fakültesi, Havacılık ve Uzay Mühendisliği Bölümü, 01000, Adana
[7,9]Adana Çukurova Üniversitesi, Mühendislik Fakültesi, Makine Mühendisliği Bölümü, 01000, Adana
[8]İstanbul Aydın Üniversitesi, Mühendislik Fakültesi, Makine Mühendisliği Bölümü, 34000, İstanbul
[10]İstanbul Teknik Üniversitesi, Mühendislik Fakültesi, Makine Mühendisliği Bölümü, 34000, İstanbul

[1]https://orcid.org/0000-0002-3919-6923
[2]https://orcid.org/0000-0001-8958-4687
[3]https://orcid.org/0000-0002-6592-3872
[4]https://orcid.org/0000-0002-9088-5679
[5]https://orcid.org/0000-0002-7766-8303
[6]https://orcid.org/0000-0001-5212-9170
[7]https://orcid.org/0000-0002-5180-3837
[8]https://orcid.org/0000-0003-0671-0890
[9]https://orcid.org/0000-0002-5342-7046
[10]https://orcid.org/0000-0002-9981-8034
*Sorumlu yazar: byaniktepe@osmaniye.edu.tr

Araştırma Makalesi

Makale Tarihçesi:
Geliş tarihi: 04.10.2023
Kabul tarihi:17.11.2023
Online Yayınlanma: 20.12.2023

Anahtar Kelimeler:
PIV
POD
Yarı küresel burun
Torpido benzeri geometri
Türbülanslı akış
Girdaplı akış

ÖZ

Geçtiğimiz on yılda geniş bir uygulama yelpazesine sahip su altı araçlarına ilgi artmıştır. Bu çalışmada, Myring profiline sahip ortak, torpido benzeri bir geometri etrafındaki akış özellikleri, Parçacık Görüntüleme Hız Ölçme (PIV) verilerinin Uygun Orthogonal Ayrıştırma (POD) analizi kullanılarak geometri boyuna göre tanımlanan Reynolds sayısının $\mathrm{Re} = 20000$ değerinde incelenmiştir. Bu çalışmada PIV ve Uygun Orthogonal Ayrıştırma (POD) analizleri sonucunda; anlık akım çizgisi topolojisi Ψ, anlık girdap $\omega L/U_\infty$ konturları, anlık akış yönünde hız bileşeni u/U_∞ grafikleri, çapraz akış yönünde hız bileşeni v/U_∞ grafikleri, anlık girdap $\omega L/U_\infty$ grafikleri, akış yönüne dik, anlık girdap grafikler ve zaman ortalamalı TKE grafikleri değerlendirildi ve karşılaştırıldı. Aynı zamanda PIV analizi sonucunda zaman ortalamalı akım çizgisi topolojisi $< \Psi >$ ve Zaman ortalamalı girdap $< \omega L/U_\infty >$ kontur değerleri verilmiştir. POD yöntemini kullanarak elde ettiğimiz akış özelliklerini PIV sonuçlarıyla karşılaştırdığımızda POD verilerinin genel olarak PIV sonuçlarına oldukça benzer olmasına rağmen POD analiz sonuçlarının daha düzgün bir yapıya sahip olduğu ve girdap türbülansının daha az olduğu belirlendi.

POD Analysis of Flow around Torpedo-Like Geometry with a Hemispherical Nose

Research Article

Article History:
Received: 04.10.2023
Accepted: 17.11.2023
Published online: 20.12.2023

Keywords:
PIV
POD
Hemispherical nose

ABSTRACT

There has been an increased interest in underwater vehicles for a wide range of applications over the past decade. In the current study, flow characteristics around a common, torpedo-like geometry with a Myring profile were investigated at a length-based Reynolds number of $\mathrm{Re} = 20000$ using the Proper Orthogonal Decomposition (POD) analysis of Particle Image Velocimetry (PIV) data. As a result of PIV and Proper Orthogonal Decomposition (POD) analyzes in this study; instantaneous streamline topology Ψ, instantaneous vorticity $\omega L/U_\infty$ contours,

Torpedo-like geometry
Turbulent-flow
Vortical flow

instantaneous streamwise velocity component u/U_∞ graphs, cross-streamwise velocity component v/U_∞ graphs, instantaneous vorticity $\omega L/U_\infty$ graphs, perpendicular to the flow direction, instantaneous vortex graphs and time-averaged TKE graphs were evaluated and compared. At the same time, as a result of PIV analysis, time-average streamline topology $< \Psi >$ and Time-averaged vorticity $< \omega L/U_\infty >$ contours values are given. When the flow characteristics were compared by using the obtained POD method of the PIV results, it was determined that although the POD data were generally quite similar to the PIV results, the POD analysis results had a more uniform flow structure and vortex turbulence was lessened.

To Cite: Kenan Ö., Yanıktepe B., Sekeroglu E., Ozgoren M., Akbudak E., Durhasan T., Kılavuz A., Sahin B., Akıllı H., Kavurmacıoglu LA. POD Analysis of Flow around Torpedo-Like Geometry with a Hemispherical Nose. Osmaniye Korkut Ata Üniversitesi Fen Bilimleri Enstitüsü Dergisi 2023; 6(Ek Sayı): 555-566.

1. Introduction

Flow structures surrounding an unmanned underwater vehicle (UUV) remain appealing topics for academics, as the usage of UUV in fields such as search-and-rescue, exploration, and defence has increased in recent years due to their multitasking capability. UUVs can be designed for specific tasks, however the majority of them feature a cylindrical hull with converging sterns, mainly based from Myring's (1976) profiles created for high efficiency military underwater vehicles like submarines and torpedoes. In general, streamlined elliptical noses are preferred in high velocity and surface layer applications; meanwhile, deep-water underwater vehicles utilize hemi-spherical or slender ellipsoids (Desa et al. 2006). The majority of the unmanned underwater vehicle research, is optimization studies in uniform flow conditions in terms of nose and stern geometries and hull length ratios (Evans and Nohan, 2004; Tyagi and Sen, 2006; Jagadeesh et al. 2009; Dantas and Barros, 2013). The maneuverability of the underwater vehicles in uniform flow is often studied for large pitching angles of attack in order to provide useful data for gliders, water to surface, and surface to water torpedoes. Lower angles of attack studies (de Barros et al., 2008; Yagmur, 2016), on the other hand, are often used in combined yawing angles of attacks studies as well as in self-adjusting route of autonomous underwater vehicles (AUVs). Experimental investigations of a torpedo-like geometries for different angles of attack and submersion ratios were performed by Kilavuz et al. (2022a, 2022b and 2022c) and Sariguzel et al. (2022). They emphasized that free-surface has a dominant effect when the submersion ratio is less than a diameter of the geometry and the elliptical noses provide a better performance near the surface. The investigation of flow characteristics, particularly the vortex structures in turbulent wakes is essential in both the cruising flow optimization and maneuverability studies.

Proper Orthogonal Decomposition (POD), first introduced in turbulence studies by Lumley (1967), is an effective method for identifying features in turbulent flow (Berkooz et al. 1993). POD extracts the coherent structures from the experimental data then provides modes in order of their contribution to the energy of the flow with "mode 1" being the largest contributor. While there are various methods to obtain the modes, this study uses the snapshot POD method introduced by Sirovich (1987) which has been commonly used by many researchers (Noack et al., 2010; Wei et al., 2016; Durhasan 2020). POD analysis has been used as a powerful postprocessing tool to identify dominant coherent flow patterns and to construct reduced order flow models that capture the largest amount of energy with the smallest

number of modes. When the flow is dominated by large-scale convective structures, as is the case in the vortex shedding studied, POD modes are found to occur in pairs that represent the orthogonal components of the harmonics of the vortex-shedding process as stated by Yang et al. (2021). Researchers studied the flow characteristics of torpedoes under uniform flow conditions (Kenan et al., 2022a; Kenan et al., 2022c; Kenan et al., 2023; Akbudak et al., 2022a, Akbudak et al. 2022b).

In the current study, snapshot POD method was employed to the experimental PIV data at Re=20000 in order to reveal coherent flow structure around the around the torpedo-like geometry under uniform flow conditions. The obtained flow characteristics from POD analysis such as the instantaneous velocity and vortical structure fields, streamlines and the time-averaged turbulent kinetic energy (TKE) taken at vertical rakes were compared to the PIV data. The chosen hemispherical nose was found to be well suited for deep water applications, and the presented findings can be utilized to verify the numerical setup by presenting high energy spots within the wake to focus on.

2. Material and Methods

The profile of the used underwater vehicle along with Myring equations is provided in Figure 1. The nose, hull, and stern lengths of the model are $L_N = 20$ mm, $L_H = 100$ mm and $L_S = 80$ mm, respectively while it has a diameter of $D = 40$ mm. The nose section is simply a hemisphere and the stern profile is given in Equation 6, where the angular parameter of the stern, θ, was taken as $\theta \cong 30°$.

$$r_S(x) = \frac{1}{2}D - \left[\frac{3D}{2{L_S}^2} - \frac{tan\theta}{L_S}\right](x - L_N - L_H)^2 + \left[\frac{D}{{L_S}^3} - \frac{tan\theta}{{L_S}^2}\right](x - L_N - L_H)^3 \quad (6)$$

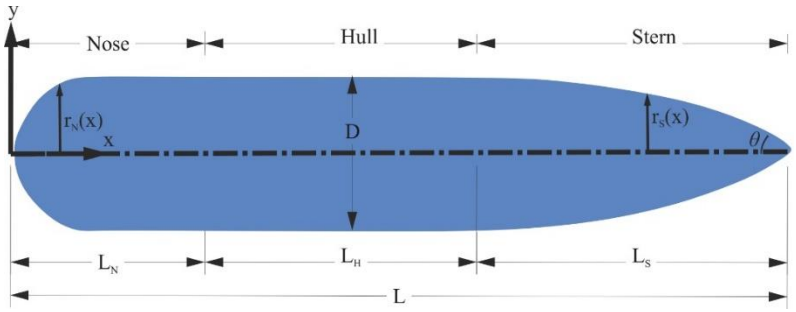

Figure 1. Parameters of the Myring profile showed on the used underwater vehicle geometry.

The Particle Image Velocimetry (PIV) technique provides quantitative data on the flow features. PIV measurements were carried out in the Advanced Fluid Mechanics PIV laboratory of Osmaniye Korkut Ata University using a 1000×800 mm^2 rectangular cross-sectioned closed-loop water channel. The water height in the channel was kept at 800 mm. A Dantec PIV system consisting of a 532 nm Nd: YAG laser source, CCD camera, and a synchronizer was used to acquire a total of 1000 double-framed images in 15 Hz frequency. The time interval between the frames was taken as approximately 8 ms. The velocity field of 7326 (99×74) vectors was obtained from the cross-correlating movement of the

illuminated 10 μm suspended seed particles between the frames of a single image. 32×32 pixel interrogation windows were using the cross-correlation algorithm with a 50% overlap. The schematic of the experimental setup and considered field of views (FoVs) are provided in Figure 2. The magnitude of uncertainty was found to be less than 2% considering the non-homogeneous seeding particle distribution, out of plane motion and noise, (Westerweel 1994; Ozgoren 2006), and more detailed information was cited therein.

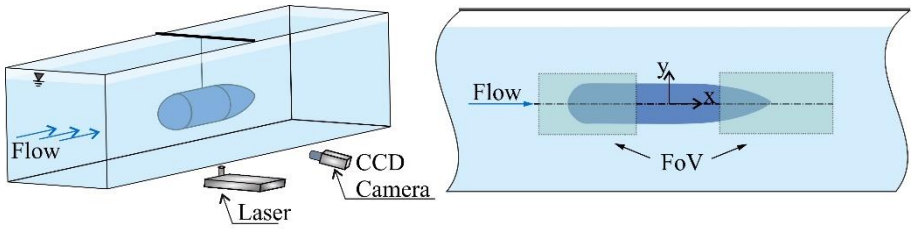

Figure 2. Sketch of experimental setup

Proper Orthogonal Decomposition is a powerful method for system description that aims to obtain low-dimensional approximate descriptions for multidimensional systems. POD provides a basis for modal decomposition of a system of functions, as do data obtained through experiments. It provides an efficient way to capture the dominant components of a multidimensional system and represent it with a desired precision using a relevant set of modes, thus reducing the degree of the system. POD consists of two parts that take a "snapshot" of a data sequence and then "mirror" the data through various modes (Anonymous, 2016).

The basic principles of the POD were briefly provided by Wang et al. (2014) as follows; first, the mean velocity field is removed from instantaneous snapshots. Equations 1-5 on the fluctuating velocity components, $u = (u, v)$ where u and v are the fluctuating velocities. Fluctuating velocity components from N snapshots are then arranged in a matrix U as $U = [u^1 u^2 \dots u^N]$. Then, an autocovariance matrix, *C*, is created as $C = U^T$ and,

$\tilde{C} A^i = \lambda^i A^i$

(1)

is solved for the eigenvalue, λ^i. The calculated eigenvalues are then ordered as:

$\lambda^1 > \lambda^2 > \cdots > \lambda^N = 0$

(2)

where the eigenvalues represent the portion of the total energy for each mode. The normalized POD models, φ^i, are constructed from the projection of the eigenvectors, A^i as:

$$\varphi^i = \frac{\sum_1^N A_n^i u^n}{\|\sum_1^N A_n^i u^n\|}, \quad i = 1,2, \dots N$$

(3)

where the notation $\|.\|$is defined as

$$\|y\| = \sqrt{y_1^2 + y_2^2 + \cdots + y_M^2}$$

(4)

Each instantaneous velocity field is then expanded into a series of the POD modes with expansion coefficients (POD coefficients), a_i, for each mode. The POD coefficients are determined by projecting the fluctuating part of the velocity field onto the POD mode as i.e., $a^n = \psi^T u^n$ where $\psi = [\varphi^1, \varphi^2 \dots \varphi^N]$. The expansion of the fluctuation part of an instantaneous field is then calculated from:

$$u^n = \sum_{i=1}^N a_i^n \varphi^i \qquad (5)$$

The procedures of the snapshot POD method were outlined by Meyer et al. (2007) and Yin et al. (2019). In this study, the POD analysis has been performed by using the Dynamic Studio software of the Dantec Dynamics company (Anonymous, 2016).

3. Results and Discussion

Time-averaged streamline topology $< \Psi >$ for PIV presented in Figure 3. There are two foci points and one saddle point in the wake region. These points F_1; $x/D = 2.51$, $y/D = 0.23$, F_2; $x/D = 2.54$, $y/D = -0.23$ and S; $x/D = 2.9$, $y/D \cong 0$ are in position. In other words, it is seen that a symmetrical structure is formed according to the center line. Both foci points are located within separation bubbles, and the vortex shedding seems to be alternating between the upper and lower shear layers in a regular manner to create a symmetric time-averaged streamline topology. Time-average vorticity $< \omega L/U_\infty >$ contours for PIV presented in Figure 4. It has been observed that the torpedo-like geometry extends downstream in the wake region of the lower and upper shear layers. It was observed that positive and negative contours were formed and a symmetrical structure was formed.

Instantaneous streamline topology Ψ for PIV and POD presented in Figure 5. As a result of PIV analysis, there are 4 foci points and 3 saddle points. These points F_1; $x/D = 2.42$, $y/D = 0.29$, F_2; $x/D = 2.31$, $y/D = -0.29$, F_3; $x/D = 2.48$, $y/D = 0.10$, F_4; $x/D = 3.09$, $y/D = -0.04$, S_1; $x/D = 2.67$, $y/D = 0.29$, S_2; $x/D = 2.31$, $y/D = -0.29$ and S_3; $x/D = 2.48$, $y/D = 0.10$ are in position. As a result of POD analysis, there are 4 foci points and 2 saddle points. F_1; $x/D = 2.29$, $y/D = 0.29$, F_2; $x/D = 2.27$, $y/D = -0.27$, F_3; $x/D = 2.61$, $y/D = -0.13$, F_4; $x/D = 3.12$, $y/D = -0.06$, S_1; $x/D = 2.62$, $y/D = -0.22$ and S_2; $x/D = 3.00$, $y/D = 0.06$ are in position. Instantaneous vorticity $\omega L/U_\infty$ contours for PIV and POD presented in Figure 6. While it was

observed that more turbulent vorticity structures were formed as a result of PIV analysis, it was observed that smoother vorticity structures were formed as a result of POD analysis.

Figures 8 and 9 give a presentation of the vertical rakes to show the distributions of the pointwise variations of the instantaneous and time-averaged PIV data alongside the POD results which further depict the main structures of the flow. Comparison of instantaneous streamwise velocity component u/U_∞, cross-streamwise velocity component v/U_∞ and instantaneous vorticity $\omega L/U_\infty$ along the stations shown in Figure 7 for PIV and POD presented in Figure 8. When looking at the instantaneous streamwise velocity component u/U_∞; In both cases, it was observed that the reverse flow region occurred at $x/D = 2.5$ and $x/D = 3.0$ stations, but did not occur at $x/D = 3.5$ station. While more turbulent results are obtained for PIV analysis, it can be seen that the POD analysis results form a symmetrical structure. When looking at the instantaneous cross-streamwise velocity component v/U_∞; While the PIV analysis result was seen to be more turbulent at the $x/D = 2.5$ station, the POD analysis result was more smooth. At all stations, the maximum and minimum points of the PIV analysis were higher than the POD analysis result. When looking at the instantaneous vorticity $\omega L/U_\infty$; While it was observed that more turbulent vorticity structures were formed as a result of PIV analysis, it was observed that smoother vorticity structures were formed as a result of POD analysis. At the same time, it was observed that as the x/D aperture ratio increased, the min-max vorticity values in the line graphs decreased and turned into an asymmetric structure. In addition, at x/D=3.5, it is seen in the dotted line graph that the POD and PIV graphs are quite close in the instantaneous vorticity value. Time-average TKE distributions $< TKE/U_\infty^2 >$ across the stations shown in Figure 7 for PIV and POD presented in Figure 9. As a result of PIV analysis, TKE values were higher for all stations. For both PIV and POD analysis results, it is seen that TKE values increase with increasing station distances. When we look at the maximum TKE values at $x/D = 3.5$, it is seen that it is 0.016 for PIV analysis and 0.015 for POD analysis.

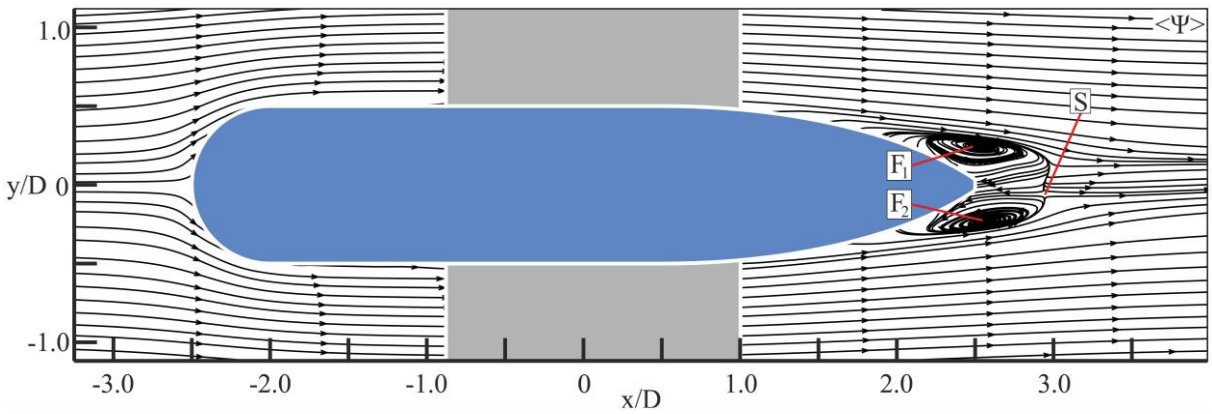

Figure 3. Time-averaged streamline topology $< \Psi >$ for PIV

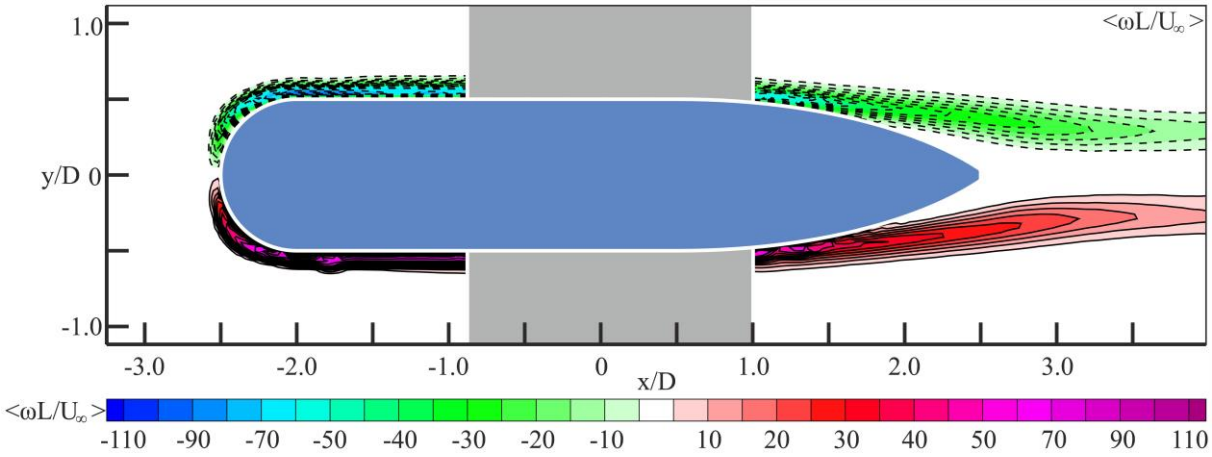

Figure 4. Time-averaged vorticity $< \omega L/U_\infty >$ contours for PIV

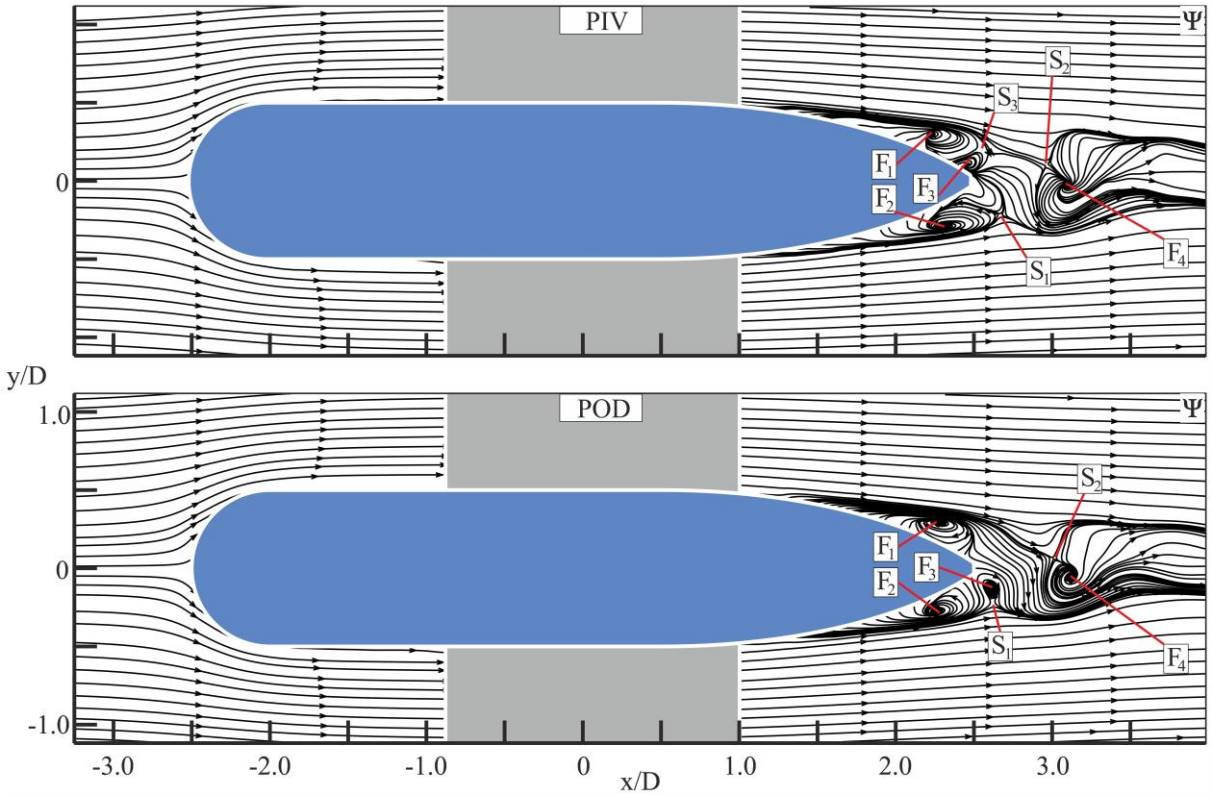

Figure 5. Instantaneous streamline topology Ψ for PIV and POD

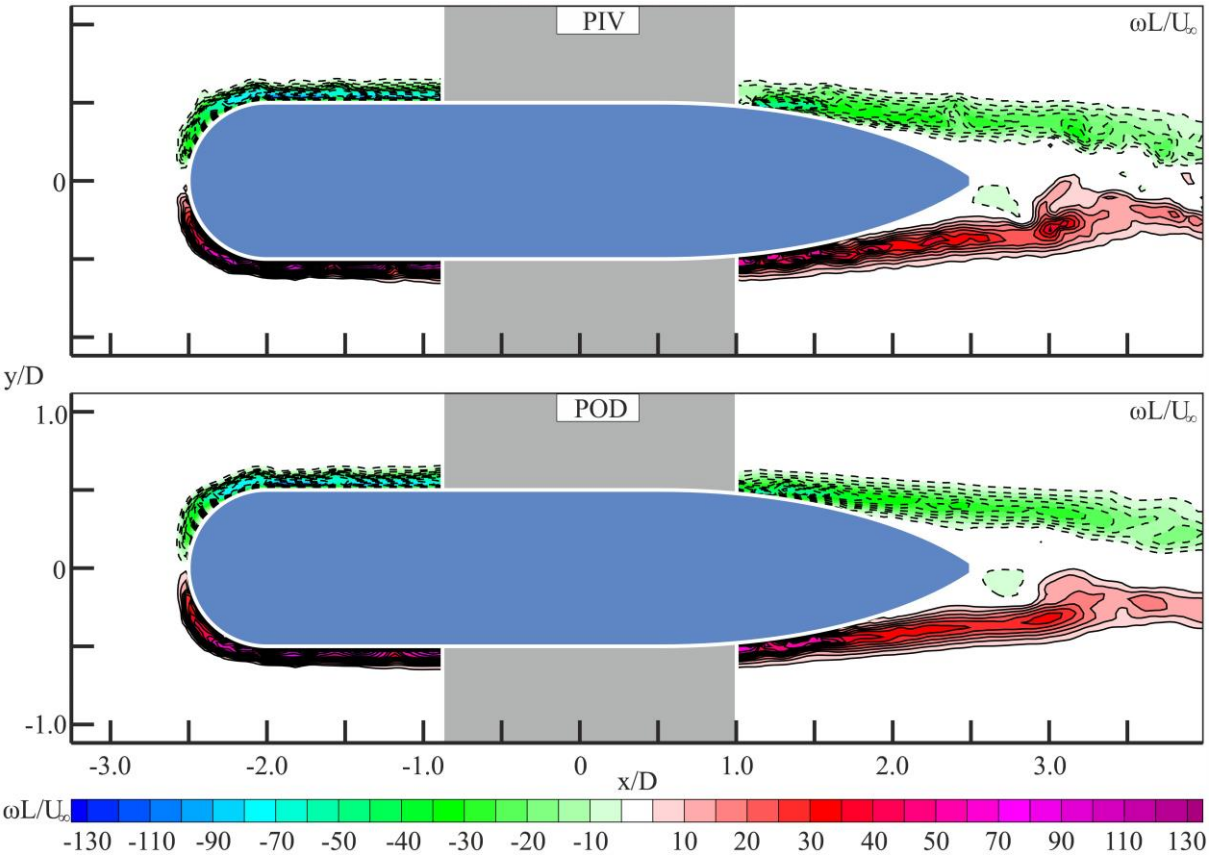

Figure 6. Instantaneous vorticity $\omega L/U_\infty$ contours for PIV and POD

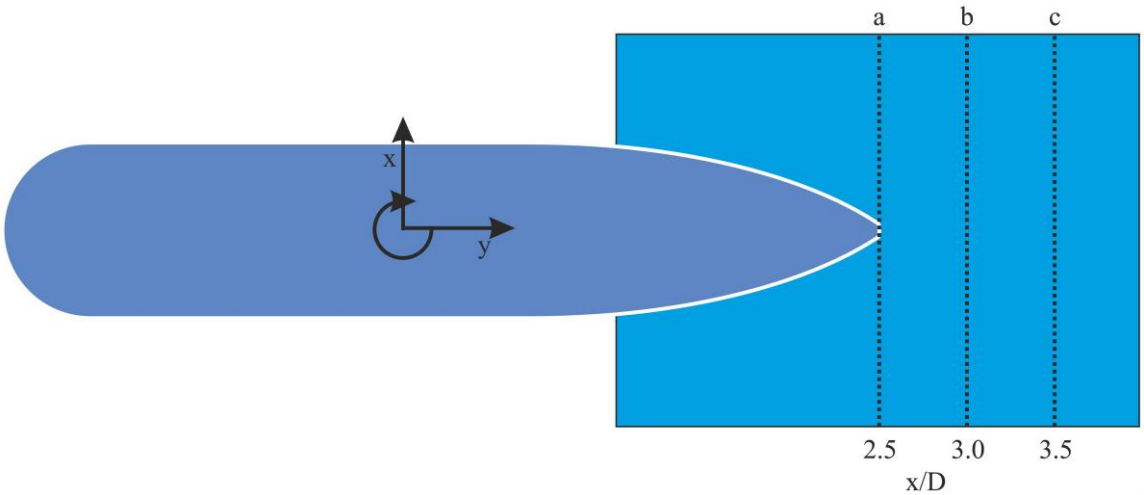

Figure 7. Present presentation of the vertical rakes to show the derived of the pointwise variations of the instantaneous and time-averaged PIV along with POD data in Figures 8 and 9

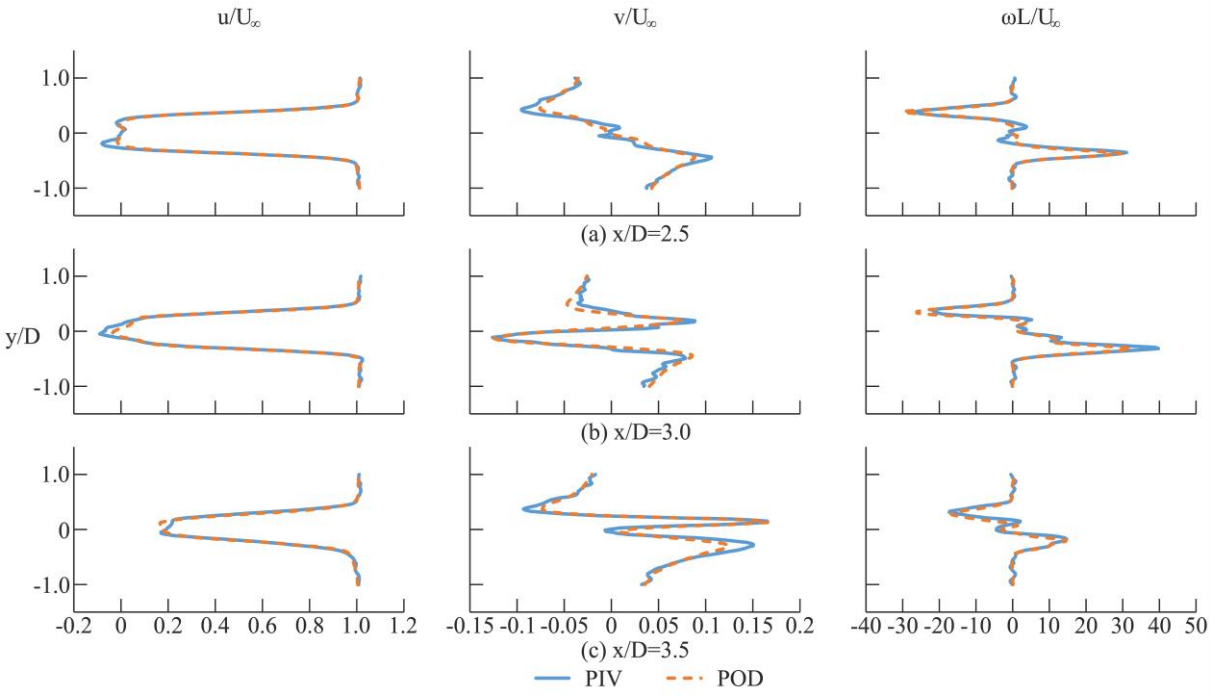

Figure 8. Comparison of instantaneous streamwise velocity component u/U_∞, cross-streamwise velocity component v/U_∞ and instantaneous vorticity $\omega L/U_\infty$ along the stations shown in Figure 7 for PIV and POD

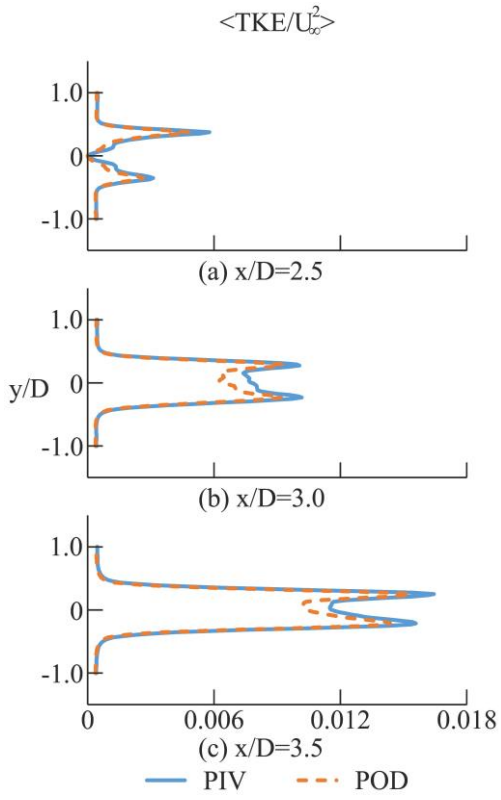

Figure 9. Time-averaged TKE distributions $< TKE/U_\infty^2 >$ across the stations shown in Figure 7 for PIV and POD

4. Conclusion

As a result of PIV and POD analyzes in this study; instantaneous streamline topology Ψ, instantaneous vorticity $\omega L/U_\infty$ contours, instantaneous streamwise velocity component u/U_∞ graphs, cross-streamwise velocity component v/U_∞ graphs, instantaneous vorticity $\omega L/U_\infty$ graphs, perpendicular to the flow direction, instantaneous vortex graphs and time-averaged TKE graphs were evaluated and compared. At the same time, as a result of PIV analysis, time-average streamline topology $< \Psi >$ and Time-averaged vorticity $< \omega L/U_\infty >$ contours values are given.

The POD method provide the data to outline, focus and study the dominant flow characteristics. When the flow characteristics of the POD data were compared to the PIV results, it was discovered that, while the POD data were generally relatively similar to the PIV results for a torpedo-like geometry cruising at α=0˚ under uniform flow conditions. Furthermore, the POD analysis depicted less vortex turbulence by focusing on the dominant wake structures.

It has been observed that as the x/D opening ratio increases, the reverse flow region for instantaneous streamwise velocity component u/U_∞ gradually decreases and ends completely at $x/D = 3.5$. At the same time, it was observed that as the x/D aperture ratio increased, the min-max vorticity values in the line graphs decreased and turned into an asymmetric structure. In addition, at $x/D = 3.5$, it is seen in the dotted line graph that the POD and PIV graphs are quite close in the instantaneous vorticity value. In future, more detail analysis will be performed for POD analysis at different angles of attack.

Acknowledgment

The authors would like to acknowledge the Scientific and Technological Research Council of Turkey (TUBITAK) under Contract No. 214M318 and thank the Advanced Fluid Mechanics PIV laboratory of Osmaniye Korkut Ata University, Turkey for using the water channel and measurement systems. In addition, the authors thank the OKU Scientific Research Projects Unit for their support with the project number OKÜBAP-2022-PT2-033 and OKÜBAP-2022-PT2-043.

References

Anonymous. Dynamic Studio software of the Dantec Dynamics, https://www.dantecdynamics.com (Access 13.11.2023), 2016.

Akbudak E., Yanıktepe B., Şekeroğlu E., Kenan Ö., Ozgoren M. Investigation of the flow structures for two tandem arrangement of torpedo-like geometries. Osmaniye Korkut Ata Üniversitesi Fen Bilimleri Enstitüsü Dergisi 2022a; 1(5): 135-155.

Akbudak E., Şekeroğlu E., Yaniktepe B., Kenan Ö., Özgören M. Investigation of flow characteristics around a blunt nose and conical stern geometry with single and tandem arrangements. UNEC Journal of Engineering and Applied Sciences 2022b; 2(2): 49-55.

Berkooz G., Holmes P., Lumley JL. The proper orthogonal decomposition in the analysis of turbulent flows. Annu Rev Fluid Mech 1993; 25: 539-575.

de Barros EA., Dantas JLD, Pascoal AM. de S ´a E. Investigation of normal force and moment coefficients for an AUV at nonlinear angle of attack and sideslip range. Journal of Oceanic Eng 2008; 33(4): 538-549.

Desa E., Madhan R., Maurya P. Potential of autonomous underwater vehicles as new generation ocean data platforms. Current Science 2006; 90(9): 1202-1209.

Durhasan T. Flow topology downstream of the hollow square cylinder with slots. Ocean Eng, 2020; 209: 107518.

Kilavuz A., Ozgoren M., Kavurmacioğlu LA., Durhasan T., Sarigiguzel F., Sahin B., Akilli H., Sekeroglu E., Yaniktepe B. Flow characteristics comparison of PIV and numerical prediction results for an unmanned underwater vehicle positioned close to the free surface. Applied Ocean Research 2022a; 129: 103399.

Kilavuz A., Durhasan T., Ozgoren M., Sarigiguzel F., Sahin B., Kavurmacioğlu LA., Akilli H., Sekeroglu, E., Yaniktepe B. Influence of free-surface on wake flow characteristics of a torpedo-like geometry. Journal of Marine Science and Technology 2022b; 27(3): 1130-1147.

Kilavuz A., Sarigiguzel F., Ozgoren M., Durhasan T., Sahin B., Kavurmacioğlu LA., Akilli H., Sekeroglu E., Yaniktepe B. The impacts of the free-surface and angle of attack on the flow structures around a torpedo-like geometry. European Journal of Mechanics-B/Fluids 2022c; 92: 226-243.

Kenan O., Yanıktepe B., Sekeroglu E., Akbudak E., Ozgoren M. Experimental investigation of instantaneous flow properties around a hemispherical nose torpedo-like geometry exposed to üniform flow. 4. International Baku Scientific Research Congress, 30 November-01 December 2022a, page number:542-551, Baku.

Kenan O.,Yanıktepe B., Sekeroglu E., Akbudak E., Ozgoren M. Experimental investigation of instantaneous flow properties around a cambered nose torpedo-like geometry exposed to üniform flow. 3. International Cappadocia Scientific Research Congres, 11-12 December 2022b, page number: 884-894, Nevşehir.

Kenan O.,Yanıktepe B., Sekeroglu E., Akbudak E., Ozgoren M. Experimental investigation of instantaneous flow properties around a hemispherical nose, 3-wing torpedo-like geometry positioned in smooth flow conditions. 1. Uluslararası Boğaziçi Bilimsel Çalışmalar Kongresi, 13-14 May 2023, page number:444-454, İstanbul.

Kumley JL. The structure of inhomogeneous turbulent flow. In: Yaglom AM, Tatarski VI (eds) Atmospheric turbulence 1967.

Meyer KE., Pedersen JM., Ozcan O. A turbulent jet in crossflow analysed with proper orthogonal decomposition. J. Fluid Mech 2007; 583: 199–227.

Myring, DF. Theoretical study of body drag in subcritical axisymmetric flow 1976; 27: 186–194.

Noack BR., Morzynski M., Tadmor G. Reduced-order modeling for flow control. CISM courses and lectures. No. 528. Springer; 2010.

Sarigiguzel F., Kilavuz A., Ozgoren M., Durhasan T., Sahin B., Kavurmacioğlu LA., Akilli H., Sekeroglu E., Yaniktepe B. Experimental investigation of free-surface effects on flow characteristics of a torpedo-like geometry having a cambered nose. Ocean Engineering 2022; 253: 111174.

Ozgoren M. Flow structure in the downstream of square and circular cylinders. Flow Meas Instrum 2006; 17: 225–235.

Sirovich L. Turbulence and the dynamics of coherent structures. III. Dynamics and scaling. Q. Appl. Math 1987; 45: 583-590.

Wang HF., Cao HL., Zhou Y. POD analysis of a finite-length cylinder near wake. Exp. Fluids 2014; 55: 1790

Wei Z., Zang B., New TH., Cui YD. A proper orthogonal decomposition study on the unsteady flow behaviour of a hydrofoil with leading-edge tubercles. Ocean Engineering 2016; 121: 356-368.

Westerweel J. Efficient detection of spurious vectors in particle image velocimetry data. Exp Fluids 1994; 16(3-4): 236–247.

Yagmur S. Investigated of flow structure around torpedo like geometries. Selçuk University Institute of Science and Science Master's Thesis, page number:154, Konya, Türkiye, 2016.

Yang Y., Probsting S., Liu Y., Zhang H., Li C., Li Y. Effect of dual vortex shedding on airfoil tonal noise generation. Phys. Fluids 2021; 33: 075102.

Yin S., Fan Y., Sandberg M., Li Y. PIV based POD analysis of coherent structures in flow patterns generated by triple interacting buoyant plumes. Build and Environ 2019; 158: 165-181.